A R C H I V E S O F M E T A L L U R G Y A N D M A T E R I A L S
Volume 58 2013 Issue 4
DOI: 10.2478/amm-2013-0132

B. LESZCZYŃSKA-MADEJ*, M. RICHERT*

THE EFFECT OF DYNAMIC COMPRESSION ON THE EVOLUTION OF MICROSTRUCTURE IN ALUMINIUM AND ITS ALLOYS

WPŁYW DYNAMICZNEGO ŚCISKANIA NA MIKROSTRUKTURĘ ALUMINIUM I JEGO STOPÓW

In the work, the microstructure and selected properties of aluminium and its alloys (AlCu4Zr0.5, AlMg5, AlZn6Mg2.5CuZr) deformed with high strain rate were investigated. The cylindrical samples were compressed by a falling – weight-type impact-testing machine at the strain rate ranging from 1.77-6.06×10^2 s^{-1} in order to attain true strains between ϕ = 0 - 0.62. After compression, the microhardness of the samples was tested and the microstructure was examined by means of both optical (LM) and transmission electron microscopy (TEM). Additionally the misorientation of selected microstructural elements using proprietary KILIN software was determined. The large density of shear bands, bands and microbands was the characteristic feature of the microstructure. The statistical width of the microbands observed in the microstructure was calculated using the mean chord method. The obtained data demonstrate reduction of the microbands width with the increase of deformation. The main object of investigations concerns the microstructure elements refinement affected by dynamic compression.

Keywords: aluminium alloys, microstructure, ultrafine grained microstructure, nanocrystalline microstructure, transmission electron microscopy (TEM)

W pracy przedstawiono wyniki badań mikrostruktury i wybranych właściwości polikrystalicznego aluminium i jego stopów: AlMg5, AlCu4Zr0.5, AlZn6Mg2.5CuZr ściskanych dynamicznie za pomocą młota spadowego. Próbki odkształcano w zakresie odkształceń rzeczywistych ϕ = 0-0.62 z prędkością odkształcenia z zakresu 1.77-6.06×10^2 s^{-1}. Na tak odkształconych materiałach przeprowadzono pomiar mikrotwardości oraz badania mikrostruktury przy zastosowaniu transmisyjnego mikroskopu elektronowego (TEM) i mikroskopu świetlnego (LM), dodatkowo przeprowadzono pomiar dezorientacji w mikroobszarach metodą linii Kikuchiego przy zastosowaniu oprogramowania KILIN.

Cechą charakterystyczną mikrostruktury badanych materiałów były licznie obserwowane pasma i pasma ścinania. Wyniki uzyskane przy zastosowaniu transmisyjnego mikroskopu elektronowego dowiodły występowania licznych mikropasm i mikropasm ścinania, które w zależności od materiału przebiegały na tle różnych układów dyslokacyjnych. Obserwowane mikropasma wykazywały dużą dezorientację względem osnowy. Stwierdzono wzajemnie przecinanie się mikropasm. W zakresie wyższych wartości odkształcenia, mikropasma wypełniały niemal całą objętość próbek. Zaobserwowano zależność zmniejszania się średniej szerokości i mikropasm wraz ze wzrostem wielkości odkształcenia i prędkości odkształcenia.

Praca miała na celu określenie wpływu prędkości odkształcenia (1.77×10^1 – 6.06×10^{2}s^{-1}) na możliwość rozdrobnienia mikrostruktury polikrystalicznego aluminium Al99.5 i jego stopów (AlMg5, AlCu4Zr0.5, AlZn6Mg2.5CuZr) odkształcanych w procesie dynamicznego ściskania za pomocą młota spadowego.

1. Introduction

The required properties of the materials depend among others on the production method. One of the group of the methods which allows obtaining material with high strength properties and ultrafine – grained (UFG) and even nanostructure with the grain size below 100 nm, are the Severe Plastic Deformation (SPD) methods. The possibility of producing bulk nanomaterial by SPD methods depends among other on the kind of the initial material, amount of deformation, strain rate, existence of second phases and value of the stacking fault energy. Nanostructures in steels, copper, titanium, zirconium, uranium and their alloys were found after forming by means of SPD methods. The comparison of different materials shows that with the increase of stacking fault energy the material is less susceptible for nanostructure formation. The aluminium is an example of such behavior. The high value of the stacking fault energy of Al leads to the easy structural recovering, preventing the formation of nanostructures [1-7]. The bulk nanometric or ultrafine grained materials achieve new and extraordinary properties different than obtained in the same materials produced by a conventional process of plastic deformation. They have not only very small grain size but also specific defect structures, high internal stress, crystallographic texture and often change of phase composition. Also characteristic for nanomaterials is the superplasticity effect [8]. The nanostructures observed in the bulk materials, which were formed through the SPD methods, are built from typical

* AGH UNIVERSITY OF SCIENCE AND TECHNOLOGY, FACULTY OF NON-FERROUS METALS, AL. A. MICKIEWICZA 30, 30-059 KRAKÓW, POLAND

dislocation microstructures with high density of dislocations at the grain boundaries. The large surface of the grain boundaries is the reason of increasing amount of stored energy in nanometric volumes [7]. The alternative to the SPD methods is the deformation with high strain rates (10^2 – 10^6 s^{-1}). High strain rates can be applied for example by hydrostatic extrusion process, Hopkinson split bar, ballistic impact, explosive fragmentation, high – speed shaping and forming or dynamic compression. The results obtained from the investigations with the high strain rates show the higher value of microhardness than obtained with static deformation and similar structural effects to those observed after application of one of the SPD methods [9]. Characteristic feature of dynamically deformed materials is activation of the deformation in the shear bands, microbands and adiabatic shear bands. Localized shear deformation in the form of narrow bands generated during the dynamic deformation under high strain rates has been a topic of a great interest for decades. Tresca had observed this phenomenon in the nineteenth century [10]. Especially interesting is the temperature effect connected with the adiabatic shear bands due to which essential changes in the microstructure were noticed [9]. Observations of the structure of the highly deformed materials show that shear bands and adiabatic shear bands strongly contribute to the formation of the nanograins, which form inside the mutually crossing microbands [7]. Inside bands which form in the conditions of the high strain rate, the nucleation of the nanograins was also observed [11]. The presented data indicate that the increase of the rate of the deformation is enough to create the similar effects as in the range of enormous strains exerted by SPD methods.

The aim of the presented study is to establish the influence of the strain rate (from the range 1.77×10^1 - $6.06\times10^2 s^{-1}$) on the possibility of microstructure refinement in Al99.5 and alloys: AlMg5, AlCu4Zr0.5, AlZn6Mg2.5CuZr dynamically compressed on the special laboratory hammer.

2. Materials and Experimental Procedures

2.1. Materials for investigation

The investigations were carried out on the polycrystalline aluminium Al99.5 and the following alloys: AlCu4Zr0.5, AlMg5 and AlZn6Mg2.5CuZr. The chemical compositions of the deformed materials are taken down in Tables 1-4.

TABLE 1

Chemical composition of the AlMg5 alloy [% weight]

Cu	Fe	Mn	Mg	Si	Ni	Ti	Cr	Zr	Pb	Na	Be	Al
0.008	0.049	0.005	5.524	0.09	0.001	0.001	0.001	0.001	0.001	0.0015	0.0012	94.31

TABLE 2

Chemical composition of the AlCu4Zr0.5 alloy [% weight]

Si	Fe	Cu	Mn	Mg	Cr	Ni	Zn	Pb	Sn	Ti	Zr	Al
0.00002	0.0224	4.21	0.00002	0.0002	0.0003	0.00003	0.02	0.002	0.005	0.0008	0.51	95.23

TABLE 3

Chemical composition of the AlZn6Mg2.5CuZr alloy [% weight]

Mn	Ti	Cr	Fe	Zr	Cu	Mg	Zn	Al
0.01	0.008	0.23	0.07	0.42	1.53	2.61	6	89.12

TABLE 4

Chemical composition of the Al99.5 [% weight]

Cu	Mg	Mn	Si	Fe	Zn	Ti	Pb	Al
0,007	0,013	0,008	0,11	0,25	0,014	0,01	0,005	99,5

TABLE 5

The conditions of annealing before the deformation process

No.	Material	Annealing temperature [°C]	Cooling conditions
1.	Al99.5	500	With furnace
2.	AlMg5	520	Water cooled
3.	AlCu4Zr0.5	540	Water cooled
4.	AlZn6Mg3CuZr	250	Water cooled

TABLE 6

Strain rates and strains obtained in the dynamic compression test

Material	ϕ	h_m [mm]	$\dot{\varepsilon}[s^{-1}]$	Material	ϕ	h_m [mm]	$\dot{\varepsilon}[s^{-1}]$
Al99.5	0	12.45	0	AlCu4Zr0.5	0	12.42	0
	0.25	8.67	$1.77x10^2$		0.23	8.88	$1.77\ x10^2$
	0.28	8.2	$2.54x10^2$		0.27	8.26	$2.48\ x10^2$
	0.30	7.96	$2.69\ x10^2$		0.36	6.97	$2.67\ x10^2$
	0.37	6.75	$2.77\ x10^2$		0.39	6.24	$3.17\ x10^2$
	0.41	6.09	$3.27\ x10^2$		0.43	5.65	$3.54\ x10^2$
	0.46	5.09	$3.63\ x10^2$		0.44	5.49	$3.91\ x10^2$
	0.62	1.7	$4.34\ x10^2$		0.50	4.22	$4.02\ x10^2$
AlMg5	0	8.55	0	AlZn6Mg2.5CuZr	0	12.47	0
	0.06	8.05	$2.58\ x10^2$		0.26	8.83	$1.76\ x10^2$
	0.2	6.7	$2.74\ x10^2$		0.30	8.16	$2.5\ x10^2$
	0.25	6.1	$3.29\ x10^2$		0.36	7.03	$2.7\ x10^2$
	0.33	5.25	$3.62\ x10^2$		0.40	6.38	$3.14\ x10^2$
	0.45	3.65	$4.21\ x10^2$		0.45	5.45	$3.46\ x10^2$
	0.49	3.19	$6.06\ x10^2$		0.48	4.72	$4.05\ x10^2$

Before the deformation, the samples were annealed in the sylite furnace during 2 hours at the conditions presented in Table 5.

2.2. Method of deformation

Cylindrical samples of the initial diameter φ_o = 10 mm and height h = 12.5 mm were compressed on a falling – weight – type impact testing machine. The scheme of the falling – weight – type impact – testing machine is presented in Fig. 1.

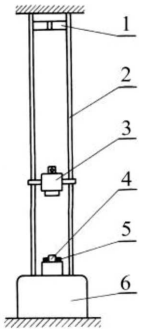

Fig. 1. Falling – weight – type impact – testing machine; 1 – beam, 2 – shears, 3 – beater, 4 – sample, 5 – distance ring, 6 – stand

The data of strain rates and strains for the compressed materials are presented in Table 6.

2.3. Microstructural characterization

After the deformation, the samples were investigated by means of both optical and transmission electron microscopy JEM 2010 ARP. The investigations by means of optical microscopy were performed on the longitudinal sections of the samples. The samples were cut out along the axis and then mechanically ground and polished using diamonds pastes (9 μm, 6 μm, 3 μm) and colloidal suspension of SiO_2. The polycrystalline aluminium Al99.5 was additionally electrolytically polished in a reagent composed of: 20% $HClO_4$+ 80% C_2H_5OH at 22V. The used technique for showing microstructure and deformations effects was etching in the Barker reagent. The composition of the Barker reagent was: 1,8 cm^3 HBF_4+100 ml H_2O. For the observations of the microstructure, the OLYMPUS GX 51 optical microscope was used with the digital recording of the image.

The thin foils for electron transmission observations were cut out from longitudinal sections of the samples and prepared applying the standard technique of electrolytic polishing using the Struers apparatus. The misorientation of selected microstructural elements was determined using proprietary KILIN software. In the case of Al99.5 and AlCu4Zr0.5 alloy, the misorientation in 35 areas was measured and the statistical data analysis was carried out for these materials. The micrographs obtained from the TEM observations were used for the calculations of the statistical width of the microbands observed in the microstructure. This was determined by the mean chord method.

To establish how dynamic compression influences the properties of the investigated materials, the microhardness was measured. The measurements were performed on the polished longitudinal sections of the samples perpendicular to the sample axis. The applied load was 100 g.

3. Results and discussion

3.1. Results obtained by using optical microscope

In order to avoid misunderstanding definitions of "bands" and "shear bands" for the need of the article should be introduced. Thus, the word "a band" concerns a band which is limited to a single grain only, whereas "shear bands" may proceed at the considerable distance and cross grain boundaries and sometimes forms distinct jogs at the intersected boundaries.

Before the deformation, the microstructure was built from the equiaxed grains. In the Al99.5, the mean width of the grain before the deformation was about 180 μm, in the aluminium alloys respectively: in AlCu4Zr0.5 alloy – 170 μm, in AlMg5 alloy – 390 μm and in AlZn6Mg2.5CuZr alloy – 45 μm. The selected microstructures obtained by using optical microscope are presented in Figures 2a-2d.

The optical micrographs, thus in the aluminium and its alloys show grains cut by the numerous bands and shear bands (Fig. 2a, 2b, 2c, 2d). Very characteristic is straight course of bands trough the sample intersecting grain boundaries (Fig. 2a, 2b, 2c, 2d). The distinct jogs were formed at the crossing boundaries (Fig. 2a, 2c, 2d). This feature allows identifying these bands as a shear bands. The bands and shear bands observed in the microstructure have diversified inclination to the compression direction. Probably this spread of the positions of bands is connected with the rotation of the material during deformation process and internal stresses.

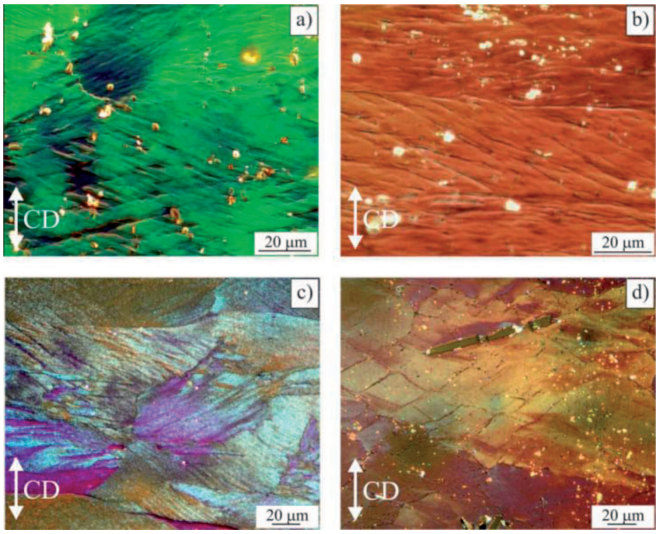

Fig. 2. Microstructures of dynamically compressed; aluminium Al99.5 – ϕ = 0.46 (a); aluminium Al99.5 – ϕ = 0.62 (b); AlMg5 alloy – ϕ = 0.49 (c), AlCu4Zr0.5 alloy – ϕ = 0.39 (d) (CD – compression direction); LM

Also characteristic features of the dynamically compressed aluminium Al99.5 and its alloys are bands intersections (Fig. 2a, 2d). This effect was observed from the small deformation, but its tremendous development appeared at higher deformations.

3.2. Results obtained by using transmission electron microscope and the misorientation measurements

The microbands and microshearbands constituted the characteristic features of dynamically compressed Al99.5 and its alloys: AlMg5, AlCu4Zr0.5, AlZn6Mg2.5CuZr (Figs. 3a-3d). Depending on the kind of the material, the microbands and microshearbands were found on a background of various dislocation structures.

A characteristic feature in the Al99.5 was occurrence of equiaxed subgrains with low dislocation density (Fig. 3a). Also characteristic was microbands existence. The observed in the Al99.5 microbands were built from elongated subgrains free of dislocations (Fig. 3a). The dislocations were observed only occasionally, in some subgrains (in spite of a changing position and inclination of thin foil. This can support the conjecture of the intense structure renewal processes. The new grains in the polycrystalline aluminium form in the neighborhood of microbands. Occasionally, cell microstructure appeared inside microbands (Fig. 3a). This cell microstructure can transform into new grains during deformation process.

In the aluminium alloys the microbands crossing the carpet – like dislocation structure were found (Figs. 3b, 3c, 3d). Additions presented in the microstructure of the alloy block dislocations' motion and therefore, the carpet – like dislocation structure forms in the entire volume of deformed samples.

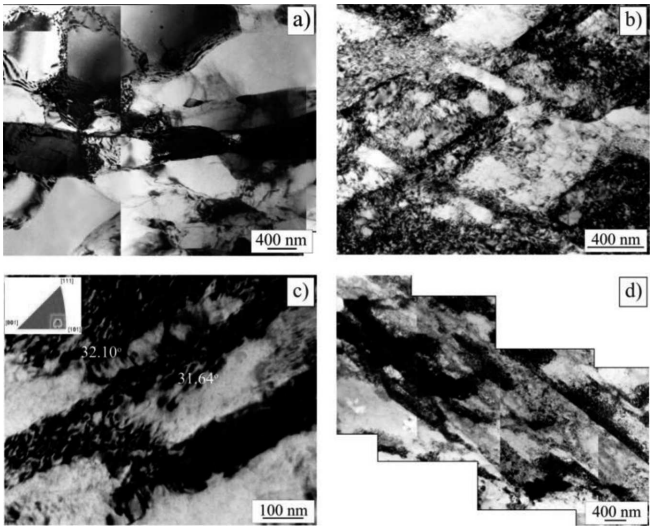

Fig. 3. Characteristic dislocations structures of dynamically compressed; aluminium Al99.5 – ϕ = 0.45 (a); AlMg5 alloy – ϕ = 0.49 (b); AlCu4Zr0.5 alloy – ϕ = 0.44 (c); and AlZn6Mg2.5CuZr alloy – ϕ = 0.49 d); TEM

The microbands are built from two parallel dislocation walls which form boundaries of the areas of considerable dislocations density. Prevailing, both the walls and interior of microbands show high dislocations density (Figs. 3b, 3c, 3d). Due to increase of deformation, the microstructure refinement and the abrupt increase of the number of the microbands occurred. Thick tangles of the microshearbands proceeding at the considerable distances were characteristic feature of microstructure (Fig. 3d). The observed shear bands could be formed by the process of adiabatic shearing affected during the dynamic compression. These bands are manifestation of a thermomechanical instability resulting in the concentration of

large shear deformations in narrow region. This strain localization is accompanied by a large local growth of the temperature which is a necessary condition to have adiabatic shearing.

In the range of higher deformations the second family of microbands was also observed intersecting the first family and forms characteristic chess – board structure (Fig. 3b). The mutually crossing microbands lead to the formation of micro – and nanovolumes, which could transform into new grains, as it was described and discussed in literature [7, 12]. A similar situation takes place in the samples deformed with enormous strains by the cyclic extrusion compression method (CEC) [7].

Common feature of all investigated alloys is large misorientation of the microbands with respect to the matrix (Fig. 3c). Small misorientation angles were observed only occasionally. The occurrence of the large misorientation angles indicate a considerable rotation of the material during the deformation and points to resemblance to phenomena appearing during the deformation with large plastic deformation exerted by the Severe Plastic Deformation Processes method (SPD) [7]. This phenomenon is also connected with considerable energy storage in the vicinity of newly created grain boundaries. In the conditions of the high strain rates this can lead to a considerable temperature rise of the whole system and the processes of structure renewal are intensified. Due to the above, the microstructures with domination of the large misorientation angles (for example produced by SPD method or dynamic compression) could be instable under elevated temperatures in the successive applications.

In Table 7 the statistical misorientation data analysis of the polycrystalline aluminium Al99.5 and AlCu4Zr0.5 alloy are presented. The results indicate that the large misorientation angles dominate. In the AlCu4Zr0.5 alloy, the characteristic feature is increase of the number of the large misorientation angles (above 15°) with the increase of deformation. After the deformation $\phi = 0.44$ a portion of large misorientation angles is about 67% whereas after deformation $\phi = 0.5$ about 83%.

TABLE 7
Quantitative changes of low and large misorientation angles for the selected deformation in the polycrystalline aluminium Al99.5 and AlCu4Zr0.5 alloy

		Fraction of misorientation angles [%]		
		Material		
		Al99.5	**AlCu4Zr0.5**	
Distribution of the misorientation angles Θ	[°]	Strain value		
		$\phi = 0.3$	$\phi = 0.44$	$\phi = 0.5$
	0 – 15	26.1	33.33	16.7
	15 – 60	73.9	66.67	83.3

The data presented in works [7, 13] showing results of ultrafine or nanograined aluminium Al99.5 and its alloys AlMg5, AlMg3 and AlCu4Zr0.5, deformed by Cyclic Extrusion Compression Method (CEC), Hydrostatic Extrusion Method (HE) and Equal Channel Angular Pressing Method (ECAP) also indicate the domination of large misorientation angles (Table 8).

TABLE 8
Quantitative changes of large misorientation angles obtained for different deformation methods in Al99.5 and AlMg5, AlMg3, AlCu4Zr0.5 alloys

Material	**Method, strain value**	**Fraction of large misorientation angles**
Al99.5	CEC, $\phi = 18$	36% [7]
	HE, $\phi = 2.31$	87,5% [own]
AlCu4Zr0.5	CEC, $\phi = 14$	55% [7]
	HE, $\phi = 1.39$	75% [own]
AlMg5	CEC, $\phi = 14$	45% [7]
AlMg3	ECAP, $\phi = 10$	80% [13]

3.3. The statistical data analysis of the mean width of microbands formed during dynamic deformation process

Essential information concerning investigated Al99.5 and its alloys: AlMg5, AlCu4Zr0.5 and AlZn6Mg2.5CuZr provided data of the mean width of microbands. The measurements were performed by using mean chord method. Exception polycrystalline aluminium Al99.5, at the beginning of deformation ($\phi = 0.2 – 0.26$), the measured width of microbands was on the level d = 210 – 230 nm. These results allow qualifying investigated alloys as ultrafine grained materials.

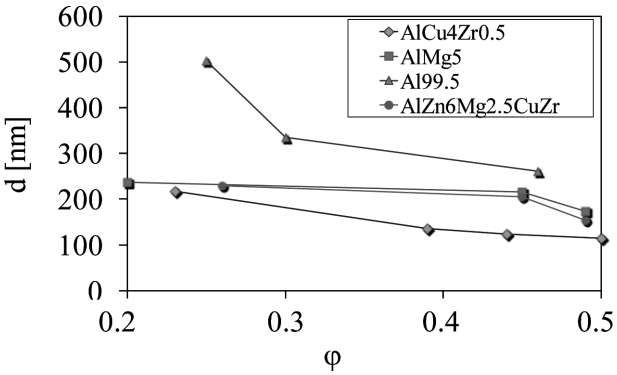

Fig. 4. The mean width of microbands as a function of strain value

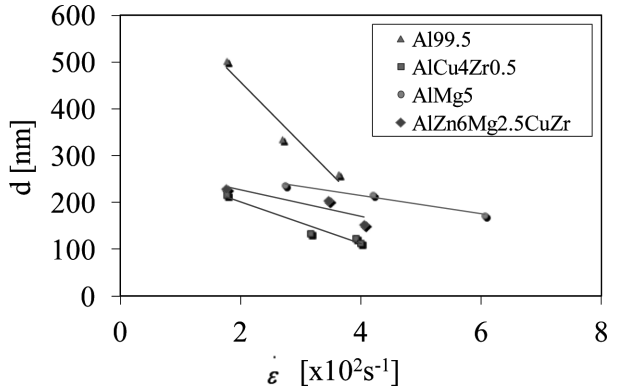

Fig. 5. The mean width of microbands as a function of strain rate

The data on measuring the mean width of the microbands demonstrate reduction of their width with increase of strain

value and strain rate. The influence of the deformation and strain rate on the diminishing width of the microbands is most significant in polycrystalline aluminium Al99.5 (Fig. 4, 5). The results obtained for this material are very promising, the mean width of the microbands after the deformation ϕ = 0.46 is about d = 260 nm. The smallest measured width of the microbands was observed in the AlCu4Zr0.5 alloy. After the deformation ϕ = 0.5 the mean width of the microbands in this alloy was about d ≈ 110 nm. In the other alloys (AlMg5, AlZn6Mg2.5CuZr) after the maximum deformation ϕ = 0.49, the mean width of the microbands is placed in the range of d = 150 – 170 nm.

The demonstrated data show that in some range the amount of the deformation and strain rate can be interchangeable causing similar structural effect. Not only severe deformations can contribute to the nanomaterials production, but also deformations with high strains rates exerted on a sample for example by dynamic compression method or hydrostatic extrusion.

4. Selected mechanical properties – microhardness

In order to investigate how dynamic compression method influences on the mechanical properties of the investigated materials, the samples were tested for microhardness. The results of micorhardness measurements are presented in Fig. 6. The results show polycrystalline aluminium Al99.5 and its alloys: AlMg5, AlCu4Zr0.5, AlZn6Mg2.5CuZr harden throughout the whole investigated range of deformation.

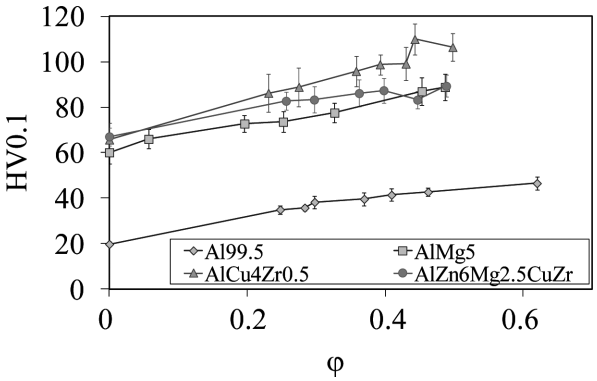

Fig. 6. The influence of the dynamic deformation on the mechanical properties of the polycrystalline aluminium Al99.5 and its alloys

In the polycrystalline Al99.5 microhardness rise from the initial level of 20 HV0.1 to the value of 45 HV0.1 after the deformation ϕ = 0.46. This material presents the lowest level of the properties. Aluminium is the material with high value of the stacking fault energy (SFE) (200 - 250 mJ/m^2). Absence of the precipitates in the materials with high value of the SFE favors easy structural recovering processes. The level of hardening for the AlMg5 and AlZn6Mg2.5CuZr alloys are comparable (fig.6). These alloys were strengthened throughout the whole investigated range of deformation attaining microhardness of 90 HV0.1 after deformation ϕ = 0.49. The increase of the properties achieve Δ = 30 HV0.1 and Δ = 23 HV0.1 for the AlMg5 alloy and for the AlZn6Mg2.5CuZr alloy, respectively. The AlCu4Zr0.5 alloy achieved the highest level of the properties from all of the investigated materials. The microhardness of this alloy was about 66 HV0.1 before the deformation. After the deformation ϕ = 0.44 it attained the level of about 110 HV0.1. Then, after the deformation ϕ = 0.5 a stabilization of the properties and even slight reduction of the properties – microhardness achieved the level of 106 HV0.1 – was observed. The monotonic hardening of these materials is caused by balance between hardening and softening processes, which have place during the dynamical compression with high strain rates. The continuous increase of microhadness indicated, that the hardening processes prevailed.

Presented dislocation microstructures in Fig. 3a-3d show that the main deformation mechanism develops by the microbands and microshearbands and it essentially contributes to the hardening. In the aluminium alloys (AlMg5, AlCu4Zr0.5, AlZn6Mg2.5CuZr) high dislocations density both in the microbands boundaries and inside the microbands was observed. An increase of deformation causes strong reduction of the microbands width. At the greatest deformations, the microbands attain the nanometric size. Some portion in the global level of sample hardening has the multiplication of the dislocations in the matrix.

Another parameter which can contribute to increase of the properties of the investigated alloys is occurrence of chess – board structure at the higher deformation (Fig. 3b). This type of microstructure is a result of intersection of the bands and microbands families.

Successive parameters having an effect on the properties are: diversifications of the alloying elements and appearance of different precipitates in these materials. In the AlCu4Zr0.5 alloy it is possible presence two types of the phases: $CuAl_2$ and $ZrAl_3$. In the AlMg alloys with magnesium contents of 4-5% Mg the Mg_5Al_8 phase appears. In cast or annealed alloys of 7xxx series the amount and phases' distribution depend on cooling rate and minor alloying elements [14]. In the AlZn6Mg2.5CuZr it is possible to find phases listed in the Table 9.

TABLE 9
Probable phases formed in AlZn6Mg2.5CuZr [14]

Alloy addition	Probable phases
Mg:Zn	$Mg_3Zn_3Al_2$ (T)
	$MgZn_2$ (η', η)
Cu, Mg, Zn	in solid solution (<1%Cu)
	in solid solution and in the Mg_2Zn_2 (η', η) phase, Al_2Cu (Θ) or $Mg_3Zn_3Al_2$ (T)
Zr	$ZrAl_3$ (in the alloys without Cr and Mn)

The microstructures obtained by using transmission electron microscopy, with EDS chemical composition analysis confirms appearance of the phases mentioned above in the investigated alloys, and are presented in Figs. 7, 8.

There are a lot of factors and parameters influenced mostly on the level of microhardness of the investigated materials. The occurrence of the different phases in these alloys stops motion of grain boundary and dislocations. Deformation localization in the narrow microbands and microshearbands found in the investigated materials can considerably increase lev-

el of the properties. The next reason of hardening could be precipitation of second phases during the thermal processing and also during the increase of temperature in the course of plastic deformation. The grain size diminishing is also important factor influencing on the aluminium and aluminium alloys microhardness level.

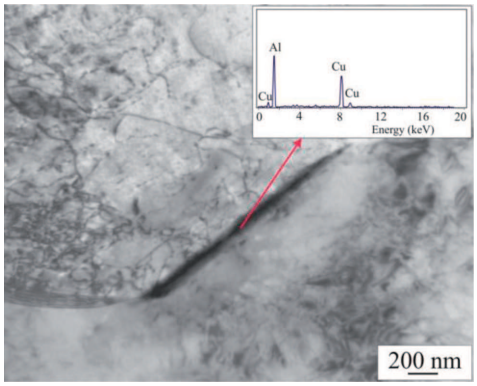

Fig. 7. Microstructures of the initial state of AlCu4Zr0.5 alloy with precipitate analysis

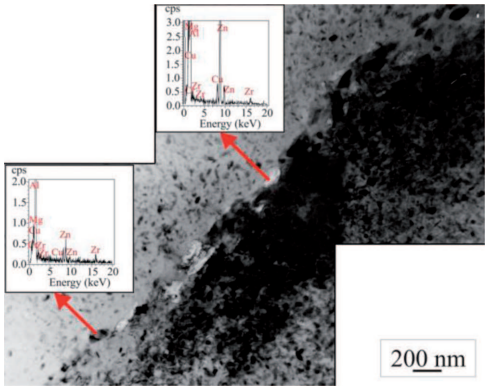

Fig. 8. Microstructures of the AlZn6Mg2.5CuZr alloy with precipitate analysis

5. Conclusions

1. The bands and shear bands has been found as a characteristic feature of microstructure of the investigated aluminium and its alloys.
2. The microbands observed in aluminium and its alloys show great misorientation (above 15°) with respect to surrounded matrix.
3. The reduction of the mean width of the microbands with increasing deformation was observed. The smallest width of the microbands d ≈ 110 nm was found in the AlCu4Zr0.5 alloy after the deformation $\phi = 0.5$.
4. Increase of deformation leads to the rise the population of the large misorientation angles (above 40°) in AlCu4Zr0.5 alloy.
5. Investigated materials harden throughout the whole investigated range of deformation.

Received: 10 April 2012.

Acknowledgements

The Statutory Activities supported this work no. 11.11.180.653.

REFERENCES

[1] M. Furakawa, Z. Horita, M. Nemoto, T.G. Langdon, Materials Science and Engineering **A 324**, 82 (2002).
[2] R.Z. Valiev, Y. Estrin, Z. Horita, T.G. Langdon, M.J. Zehetbauer, Y.T. Zhu, Journal of Materials **58/4**, 33 (2006).
[3] K.J. Kurzydłowski, Bulletyn of the Polish Academy of Science, Technical Sciences **52/4**, 301 (2004).
[4] B. Leszczyńska-Madej, M. Richert, Journal of Microscopy **237**, 399 (2010).
[5] P.B. Prangnell, J.R. Bowen, A. Gholinia, In: Proc. Of the 22nd Riso International Symposium on Mat.Sci., Science of Metastable and Nanocrystalline Alloys Structure, Properties and Modeling, (Eds.: A.R.Dinesen at al.) 105, Risø National Laboratory, Roskilde (2000).
[6] V.M. Segal, Materials Science and Engineering **A338**, 331 (2002).
[7] K.T. Park, J. Kwon, W.J. Kim, Y.S. Kim, Materials Science and Engineering **A316**, 145 (2001).
[8] M. Richert, Archive of Materials Science **26/4**, 235 (2005).
[9] M. Zhou, A.J. Rosakis, G. Ravichandran, Journal of the Mechanic and Physic of Solids **44/6**, 981 (1996).
[10] Y. Xu, J. Zhang, Y. Bai, M.A. Meyers, Metallurgical and Materials Transactions **A39**, 811 (2008).
[11] K.J. Kurzydłowski, M. Richert, B. Leszczyńska, H. Garbacz, W. Pachla, Solid State Phenomena **114**, 117 (2006).
[12] M. Richert, K.J. Kurzydłowski, Archives of Materials Science **24/4**, 561 (2003).
[13] J.S. Hayes, P.B. Prangnell, F.J. Humphreys, Materials Science Forum **331-337**, 545 (2000).
[14] L.F. Mondolfo, Aluminium alloys: Structure and Properties, London, Butterworth &Co (Publishers) Ltd 1976.